韓國精密工學會 '97年度 秋季學術大會論文集 pp.223~226

수치해석을 이용한 충격성형기계의 특성 분석
(A numerical investigation for the characterization of the impact forming machines)

Y. H. Yoo* and D. Y. Yang**
*1st R&D Center, ADD, Taejon, KOREA
**Department of Mechanical Engineering, KAIST, Taejon, KOREA

ABSTRACT

A three-dimensional elastic-plastic finite element analysis using the explicit time integration method has been performed for the characterization of the impact forming machines. The block upsetting using a forging hammer has been analyzed. The effects of machine type, work capacity of equipment and the mass ratio in an anvil-type hammer have been studied through the analysis.

1. INTRODUCTION

Such impact forging machines as forging hammers are energy-restricted machines and are the most inexpensive and versatile types of machines used in hot forging. Forging hammers are classified by the method used to drive the dies, namely, anvil-type and counterblow-type[1].

To acquire a practical information, two approaches can be taken into consideration. One approach is to conduct the precise experiment. However, it is very difficult owing to the actual problem involved in measuring the forging load and the velocity of the die under severe loading conditions. Even today published information about it is very rare[2,3]. Another approach is to simulate the impact forging process so as to know what is happening within the workpiece and dies during the impact forging process.

The purpose of this paper is to develop an efficient three-dimensional elastic-plastic finite element code using the explicit time integration method and to apply the developed finite element code to the numerical analysis for the characterization of the impact forming machines. The effects of machine type, work capacity of a forming machine and the mass ratio between the upper and lower dies in anvil-type hammer will be studied through simulation of the impact forging process.

2. EXPLICIT FINITE ELEMENT METHOD

The uncoupled finite element equation governing the motion of a material point is obtained as follows :

$$ {}^{t}F_I^{ext} - {}^{t}F_I^{int} = M_I\,{}^{t}A_I \qquad (I = 1,2,\cdots,NDOF) \qquad (1) $$

where ${}^{t}F_I^{ext}$ is the nodal force resulting from the surface traction and the body force, ${}^{t}F_I^{ext}$ is the nodal force resulting from the stress divergence term, M_I is the lumped nodal mass and NDOF is the total degree of freedom for the global system.

In order to reduce a computation time for a volume integration, the one point Gaussian quadrature is used. In a reduced interation, zero energy modes called hourglass or keystone can be generated. To prevent these modes, the hourglass resisting force is considered.

The explicit time interation scheme is conditionally stable. At each time step cycle, a time increment is calculated by the Courant stability condition. The central difference method is used to integrate the nodal variables. A contact-searching scheme based on a master-slave algorithm[4] is used to treat the contact interface and the kinematic contact condition is enforced by the penalty method[4].

3. SIMULATION CONDITIONS

In present work, the block upsetting is simulated. The block workpiece of 48mm X 48mm X 72mm height is used for the simulation and the dimensions of the block dies are 360mm X 360mm X 192mm height. For numerical simulation, the impact forging hammer with maximum work capacity of 35kJ that is a medium-size hammer is chosen[1]. The value of the friction coefficient between the workpiece and the dies is taken as 0.2[5]. The simulation is continued until the workpiece and the dies of the forging equipment are separated completely.

3.1 Modelling of the dies

It is assumed that the material response of the dies is elastic. The Young's modulus, Poisson's ratio and density of the dies made by tool steel are 211.4 GPa, 0.3 and 7.83 g/cm^3, respectively. The densities of both dies of the counterblow-type hammer and the upper die of the anvil-type hammer are scaled up by 10 times so the volume of the dies is reduced with the same ratio, while the mass of the dies is maintained constant. But the densities of the lower dies of the anvil-type hammer are scaled up by various ratios, which range from 10 times to 200 times, in proportion to the increase of the mass ratio Q. Due to the symmetry of the dies, one fourth of the dies is modelled. 180 eight-node hexahedral isoparametric elements and 294 nodal points are used for the initial mesh of each die.

For anvil-type hammer, the initial impact velocity of the upper die, V_{ia} , is calculated considering the energy balance

as follows :

$$V_{ia} = \sqrt{\frac{2E_t}{m_u}} \quad (2)$$

where E_t is the total input energy, m_u is the mass of the upper die. The initial impact velocity of the upper die calculated from equation (2) is 6(m/s). The initial velocity of the lower die is fixed to zero.

For counterblow-type hammer, the initial impact velocity of the upper and lower dies, V_{ic} , is calculated considering the energy balance as follows :

$$V_{ic} = \sqrt{\frac{2E_t}{m_u + m_l}} \quad (3)$$

where m_l is the mass of the lower die. The initial impact velocity of the upper and lower dies calculated from equation (3) is 4.24(m/s).

For the purpose of characterizing the effect of the interface between a foundation and a lower die of a anvil-type hammer, two extreme cases are considered in the simulation. The first case is a system with weak interface, where the spring constant K and the damping coefficient C are zero. The second case is a system with highly stiff interface, where K and C are infinite. The practical cases are existing between the two extreme cases. In order to model the second case properly, the following boundary condition is applied, that is, the motion of several bottom nodes of the lower die is fixed. On the other hand, in the modelling of the first case all nodes of the lower die have no constraint.

3.2 Modelling of the workpiece

In order to consider the effects of strain hardening, strain rate hardening and thermal softening, which are frequently observed in high-velocity deformation phenomena, the Johnson-Cook yield surface model[6] is applied. The experimental data of AISI 4340 steel obtained from the Johnson-Cook paper[6] are employed as material properties of the workpiece.

The forging temperature for AISI 4340 steel ranges from 850°C to 1050°C in hot working, so the mean value of the forging temperature is selected for the simulations. Due to the symmetry of the workpiece, one fourth of the workpiece is modelled. 192 eight-node hexahedral isoparametric elements and 325 nodal points are used for the initial mesh of the workpiece.

4. RESULTS AND DISCUSSIONS

4.1 Characteristics of anvil-type hammer and counterblow-type hammer

The forging simulations for the anvil-type and counterblow-type hammers with various mass ratios and interface conditions are performed. At first, the effect of mass ratio in an anvil-type hammer with weak interface is considered.

Fig. 1 shows the final deformed configurations obtained from the blow operations after the complete separation between the workpiece and the dies. It is seen here that the increase of the mass ratio results in the increase in height reduction of the workpiece. Fig. 2 shows the time histories of the forging load according to the variation of the mass ratio. The maximum forging load as well as the contact time increase with increasing mass ratio. But, this tendency is saturated at the mass ratio of 20.

To investigate the mechanism of energy transfer precisely, the proportion and the amount of energy obtained from the blow operations are illustrated in Fig. 3. When the mass ratio is increased, the plastic deformation energy is monotonically increased and the residual kinetic energy of the lower die is monotonically decreased, on the other hand, the residual kinetic energy of the upper die is abruptly changed at the mass ratio of 5. Thus, it is clearly shown that the rebounding energy of the upper die over the mass ratio of 5 is negligible in the case of the anvil-type hammer with weak interface.

Figs. 4 and 5 show the time histories of the forging load, plastic deformation energy and kinetic energy obtained from the blow operation with various conditions. It can be seen from the figures that the stiffer interface causes an increase in the maximum forging load and the contact time regardless of the mass ratio. However, the introduction of the stiff interface has a possibility to bring about transmission of severe vibration into the foundation. The results of these simulations clearly show that for the same work capacity the maximum forging load and the available plastic deformation energy obtained from counterblow-type hammer are greater than anvil-type one.

The blow efficiency η_B is defined as the ratio of the available plastic deformation energy to the input kinetic energy. Fig. 6 represents the blow efficiencies for the various impact forging conditions. The blow efficiencies for the cases with stiff interface maintain constant value without regard to the mass ratio, whereas the blow efficiencies for the cases with weak interface increase with increasing mass ratio. Because the blow efficiencies are saturated above the mass ratio of 20, for the anvil-type hammer with weak interface, it is recommended that the most suitable mass ratio is about 20. This is widely accepted in the industry. Normally, modern forging hammers show a mass ratio of 20.

4.2 Effect of work capacity

Two impact forging processes with different initial input energy are analyzed so as to examine the effect of work capacity. Using the continuous analysis technique, ten blows are calculated for anvil-type hammer with the mass ratio of 20.

Fig. 7 shows the time history of the forging load. When

the number of blow is increased, the maximum forging load obtained from each blow increases gradually. The maximum forging load obtained from the large hammer is slightly greater than small hammer. The total plastic deformation energy obtained from simulation is illustrated in Fig. 8. The plastic deformation energy obtained from the large hammer is much more than small hammer. This fact implies that the blow efficiency obtained from the large hammer is greater than the average blow efficiency obtained from the small hammer. This tendency agrees with other analytical research work[7]. The conclusion of practical significance is that large machines are intrinsically more efficient than small machines.

5. CONCLUSIONS

For the anvil-type hammer with weak interface, it has been shown that the optimal mass ratio is about 20, because the blow efficiencies are saturated above the mass ratio of 20. For the impact forging machines with the same work capacity, it has been also shown that the maximum forging load and the available plastic deformation energy obtained from counterblow-type hammer are greater than anvil-type hammer. Under the same total input energy, the maximum forging load and the total available plastic deformation energy obtained from the large hammer are greater than small hammer. Through the multi-blow forging simulation with different mass ratios, the change of the blow efficiencies and the forging loads during the blow operations has been examined. It has been shown that the increase of the mass ratio results in the increase of the forging load and the accumulated contact time.

REFERENCES

1. Lange, K. "Handbook of metal forming", 1985 (McGraw-Hill).
2. Osman, A. E. M., Sadek, M. M. and Knight, W. A. "Noise and vibration analysis of an impact forming machine", Trans. ASME, J. Eng. Ind., 1974, 233-240.
3. Gregorian, V., Sadek, M. M. and Tobias, S. A. "Noise generated by a laboratory drop hammer and its interrelation with the structural dynamics and process parameters", Int. J. Mach. Tool Des. Res., 1976, 16, 301-318.
4. Hallquist, J. O., Goudreau, G. L. and Benson, D. J. "Sliding interfaces with contact-impact in large scale Lagrangian computations", J. Comp. Meths. Appl. Mechs. Eng., 1985, 51, 101-137.
5. Schey, J. A. "Tribology in metalworking : friction, lubrication and wear", 1983 (ASM).
6. Johnson, G. R. and Cook, W. H. "A constitutive model and data for metals subjected to large strain rates and high temperature", Proc. of 7th Int. Symp. on Ballistics, 1983, 541-547.
7. Vajpayee, S., Sadek, M. M. and Tobias, S. A. "The efficiency and clash load of impact froming machines to the second order of approximation", Int. J. Mach. Tool Des. Res., 1979, 19, 237-252.

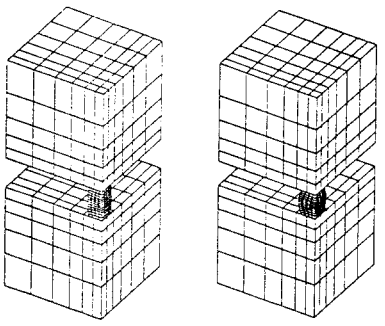

Fig. 1 Final deformed configurations obtained from the blow operations of (a) Q=1 and (b) Q=20

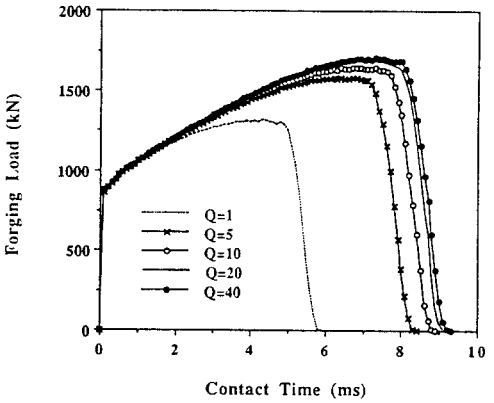

Fig. 2 Time history of the forging load obtained from the blow operations

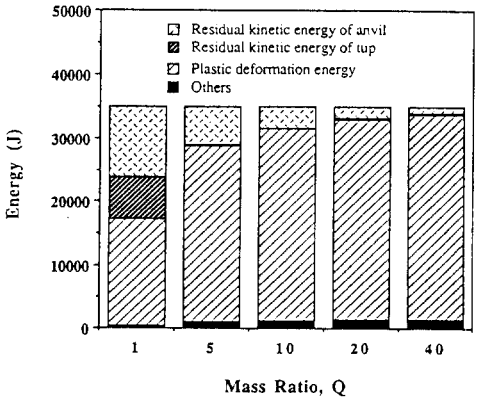

Fig. 3 Energy stack diagram obtained from the simulation

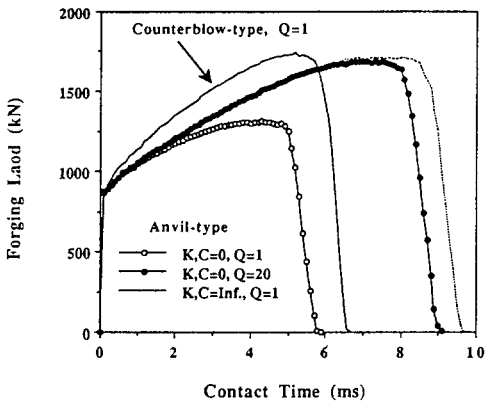

Fig. 4 Time history of the forging load obtained from the blow operation with various conditions

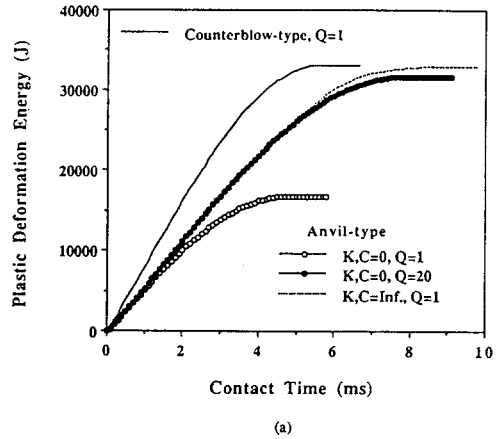

(a)

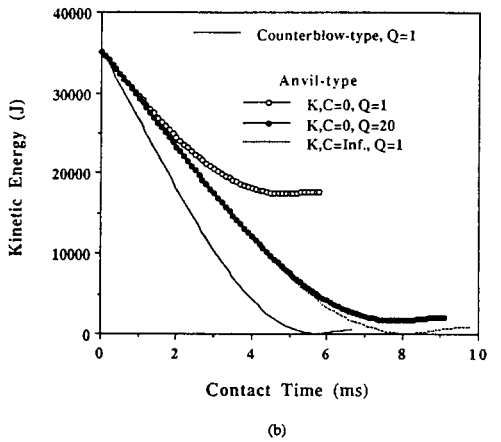

(b)

Fig. 5 Time history of (a) the plastic deformation energy and (b) the kinetic energy obtained from the blow operation with various conditions

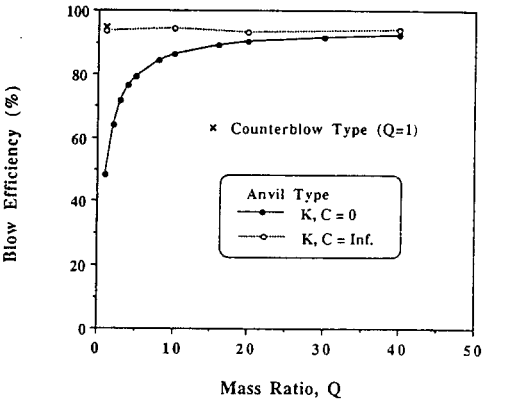

Fig. 6 Blow efficiency plot obtained from the simulation

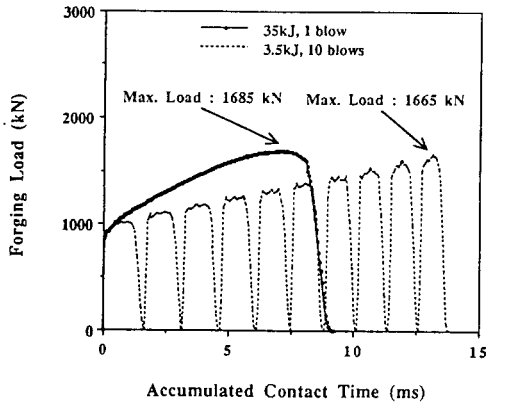

Fig. 7 Time history of the forging load obtained from the equipments with two different work capacity

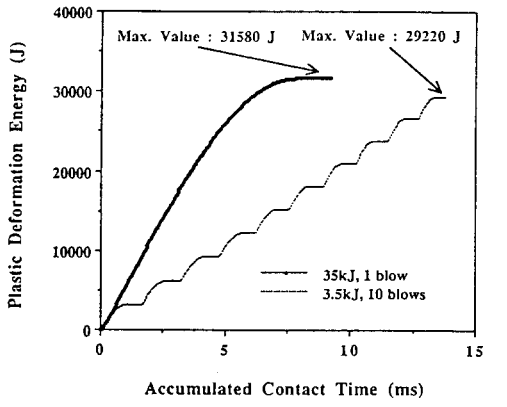

Fig. 8 Comparison of the total plastic deformation energy obtained from the equipments with two different work capacity